Simulation of Sahel drought in the 20th and 21st centuries

I. M. Held*†, T. L. Delworth*, J. Lu‡, K. L. Findell*, and T. R. Knutson*

*Geophysical Fluid Dynamics Laboratory, National Oceanic and Atmospheric Administration, ‡University Corporation for Atmospheric Research, P.O. Box 308, Princeton, NJ 08542

This contribution is part of the special series of Inaugural Articles by members of the National Academy of Sciences elected on April 29, 2003.

Contributed by I. M. Held, October 17, 2005

The Sahel, the transition zone between the Saharan desert and the rainforests of Central Africa and the Guinean Coast, experienced a severe drying trend from the 1950s to the 1980s, from which there has been partial recovery. Continuation of either the drying trend or the more recent ameliorating trend would have far-ranging implications for the economy and ecology of the region. Coupled atmosphere/ocean climate models being used to simulate the future climate have had difficulty simulating Sahel rainfall variations comparable to those observed, thus calling into question their ability to predict future climate change in this region. We describe simulations using a new global climate model that capture several aspects of the 20th century rainfall record in the Sahel. An ensemble mean over eight realizations shows a drying trend in the second half of the century of nearly half of the observed amplitude. Individual realizations can be found that display striking similarity to the observed time series and drying pattern, consistent with the hypothesis that the observations are a superposition of an externally forced trend and internal variability. The drying trend in the ensemble mean of the model simulations is attributable to anthropogenic forcing, partly to an increase in aerosol loading and partly to an increase in greenhouse gases. The model projects a drier Sahel in the future, due primarily to increasing greenhouse gases.

African drought | climate change | global warming

A fundamental goal of climate research is the creation of models that simulate the climate with sufficient realism that they can be used with confidence to predict how climate will change in the next century and beyond. We increase our confidence in our models with both holistic and reductive research. On the reductive side, we test and improve the representations of the individual physical processes that, taken together, constitute the model—radiative transfer, cloud formation, boundary layer turbulent fluxes, effects of subgrid-scale topography, mixing by unresolved mesoscale ocean eddies, and sea ice rheology, to name but a few examples. On the holistic side, we examine how the resulting model simulates the mean climate of the past few decades, its internal variability on a variety of time scales, and the emerging forced trends. When our models are unable to simulate a prominent component of the 20th century record, our confidence in their projections into the 21st century naturally is eroded.

We focus here on the remarkable variations in Sahel rainfall that occurred in the second half of the 20th century. The observed time series of wet season (July–August–September) rainfall averaged over the Sahel (10°-20°N, 20°W–40°E) is plotted as a solid black line in Fig. 1. The gridded data were obtained from the Climate Research Unit (CRU) at the University of East Anglia, Norwich, United Kingdom (version CRU-TS_2.1). A 5-year running mean was performed before plotting. See ref. 1 for a discussion of the data quality. (The region over which we average extends eastward farther than the area typically referred to as the Sahel, so as to capture northern Ethiopia as well.) The droughts of the 1970s and 1980s are well known. Less well appreciated is that the 1950s were anomalously wet as compared to the rest of the century. In the past 20 years, rainfall has recovered to values approaching the century-long mean. The spatially coherent 40% reduction in Sahel rainfall from the 1950s to the 1980s has few if any parallels in the 20th century record anywhere on Earth.

There is a body of work focusing on "desertification," land degradation not itself directly caused by climate variations and not easily reversed, as a cause of rainfall variations in the Sahel (2–5). Although there is a consensus that the Sahel is a region in which rainfall is indeed sensitive to perturbations in the land boundary conditions, it has become clear from atmospheric modeling and observational analyses begun in the 1980s that many aspects of Sahel rainfall variability are, in fact, controlled by sea surface temperatures (SSTs) (6–9). Simulations with the most recent generation of atmospheric models (10–13) have confirmed that the basic structure of the Sahel drought can be simulated when the models use the observed SSTs as a lower boundary condition. One needs to understand which patterns in the SST field force these rainfall variations and whether these SST patterns are caused by internal variability or are themselves forced externally. Our confidence in the 21st century projections for Sahel rainfall then depends in large part on the reliability of our future projections for SSTs and on our knowledge of the responses to those SSTs.

Many studies (6–14) have pointed to SST anomalies antisymmetric with respect to the equator as being of key importance for Sahel rainfall, with warmer SSTs in the Northern hemisphere (especially the north Atlantic) and colder SSTs in the Gulf of Guinea (15) and the Southern hemisphere being positively correlated with Sahel rain. Recently, special emphasis also has been placed on Indian Ocean SSTs (11, 12, 16), with the Sahel drying as the Indian Ocean warms. The Sahel is the northernmost limit of the seasonal migration of the tropical rain belt over Africa. When the Southern hemisphere warms with respect to the Northern hemisphere, one can picture the rain belt as being attracted farther south, toward the warmed hemisphere, causing the northern limit of the seasonal migration to retreat, drying the Sahel.

An appropriate null hypothesis is that most of the decadal variations in Sahel rainfall in the 20th century were generated by internal decadal variability in the SST field. But, in addition to this internal variability, there could also be an externally forced component to the observed variations. The importance of the cross-equatorial SST gradients suggests that the cooling caused by anthropogenic aerosols, which is concentrated in the Northern hemisphere, could contribute to a drying trend over the Sahel. Support for this claim comes from a climate model (14) in which an attempt is made to account for the indirect effect of

Conflict of interest statement: No conflicts declared.

Abbreviations: CRU, Climate Research Unit; SST, sea surface temperature; IPCC/AR4, Intergovernmental Panel on Climate Change Fourth Assessment.

†To whom correspondence should be addressed. E-mail: isaac.held@noaa.gov.

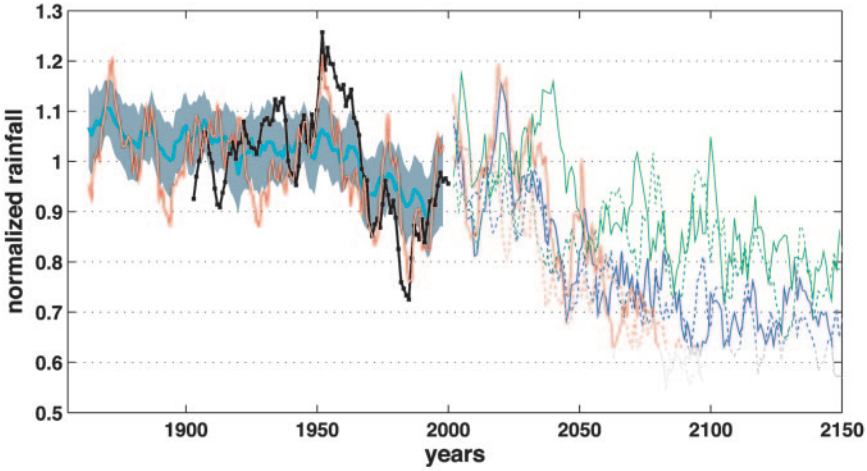

Fig. 1. Observed (CRU) 5-year running mean (July–August–September) Sahel rainfall, normalized by its mean value over 1901–2000 (black line), historical CM2 ensemble mean normalized so that its mean value is unity over the same time interval (thick light blue line), and the historical realization that most resembles the observations in the period 1950–2000 (thick red line). The gray area represents ±1 standard deviation within the ensemble. The future scenarios are B1 (green), A1B (blue), and A2 (red). There are two lines for each scenario, one from CM2.0 and another from CM2.1.

anthropogenic aerosols on clouds as well as the direct effect of the aerosols on the scattering and absorption of radiation. The indirect effect is thought to increase the magnitude of the aerosol cooling substantially. A significant response of the Sahel to the large aerosol cooling in this model is observed.

In contrast, increasing greenhouse gases, to the extent that they influence interhemispheric SST gradients at all, are expected to warm the Northern hemisphere more quickly than the Southern hemisphere. If the effect on Sahel rainfall is through the interhemispheric SST gradient, then this effect should increase Sahel rainfall. It is sometimes suggested that the recovery of the Sahel rainfall in the last two decades could be the first sign of the emergence of this greenhouse signal (17). If this signal dominates in the 21st century, we should, by this argument, expect further moistening in the Sahel. Several models simulate such a trend (18, 19). On the other hand, the results in ref. 10 suggest that the Sahel dries in some models in response to uniform warming of SSTs, with the implication that further drying in the 21st century is a possibility.

Results

We present results here for Sahel rainfall from a climate model recently developed at the Geophysical Fluid Dynamics Laboratory of the National Oceanic and Atmospheric Administration. We refer to two versions of this model (designated CM2.0 and CM2.1). For a description of both versions, and an analysis of the simulation of surface temperature trends in the 20th century that these models generate, see refs. 20 and 21. In middle and high latitudes, CM2.1 produces better positioned wind fields and smaller biases in surface temperature, but aspects of the tropical circulation, including the simulated El Niño-Southern Oscillation (ENSO) variability, are superior in CM2.0 (20, 22). Both models have been used to generate multiple realizations of 20th and 21st century climate following the protocol set by the Intergovernmental Panel on Climate Change (IPCC) for its upcoming Fourth Assessment (AR4). The two models produce similar responses in the Sahel. Neither model includes the indirect effects of aerosols on clouds, and neither includes interactive vegetation or interactive dust aerosol. The primary difference between the two models is in the numerical advection scheme in the atmosphere, but there are also significant differences in the treatment of frozen soil and subgrid scale mixing in the ocean. We refer to the set of both models as CM2.

Three integrations of CM2.0 and five of CM2.1 for the period 1860–2000 are available, forced by estimates of changes in well mixed greenhouse gases, tropospheric sulfate and carbonaceous aerosols, volcanic aerosols, ozone, solar irradiance, and land use. Single realizations of the IPCC future scenarios designated B1, A1B, and A2 are also available for each model (23); by 2100, these scenarios reach CO_2 values of ≈550, 720, and 860 ppm, respectively.

The ensemble mean and the standard deviation of the eight 20th century simulations are plotted against the observations in Fig. 1, along with the single realization that provides the best fit to the observed series over the last half of the 20th century. Just as for the observations, we average the simulated rainfall over July–August–September and over the region (10°-20°N, 20°W–40°E), and use a 5-year running mean before displaying the results. The observations and model results are both normalized by their mean over the century (the mean rainfall in CM2 in this region is 20% larger than observed). We also show the six individual 21st century simulations generated by the two models for the three scenarios.

The ensemble mean simulation shows a drying trend over the second half of the 20th century, with a hint of recovery near the present. The model's mean drying trend over 1950–2000 is 14%/50 years. Based on 500-year control simulations with both models, we estimate that the width of the 95% confidence interval for an eight-member ensemble mean of 50-year trends is ± 3–4%. Therefore, this ensemble mean trend is primarily the response of the model to varying external forcing rather than internal variability.

If we consider CM2.0 and CM2.1 separately, we find that the CM2.0 ensemble mean moistens the Sahel over the first 50 years of the 20th century, as in the observations, whereas the CM2.1 ensemble mean dries more continuously over the century. A larger ensemble would be needed to determine whether this distinction between CM2.0 and CM2.1 is significant or due to sampling of internal variability. The observed drying trend is 39% over 1950–2000 and 14% over the full century, as compared to the corresponding figures averaged over the full CM2 ensemble of 14%/50 years and 13%/100 years. The latter figure happens to be similar to that in the observations, but it is clear from Fig. 1 that the observed trend is very sensitive to the endpoints of the interval chosen.

As seen in Fig. 1, the realization that best fits the observations (one of the CM2.0 integrations) happens to generate droughts

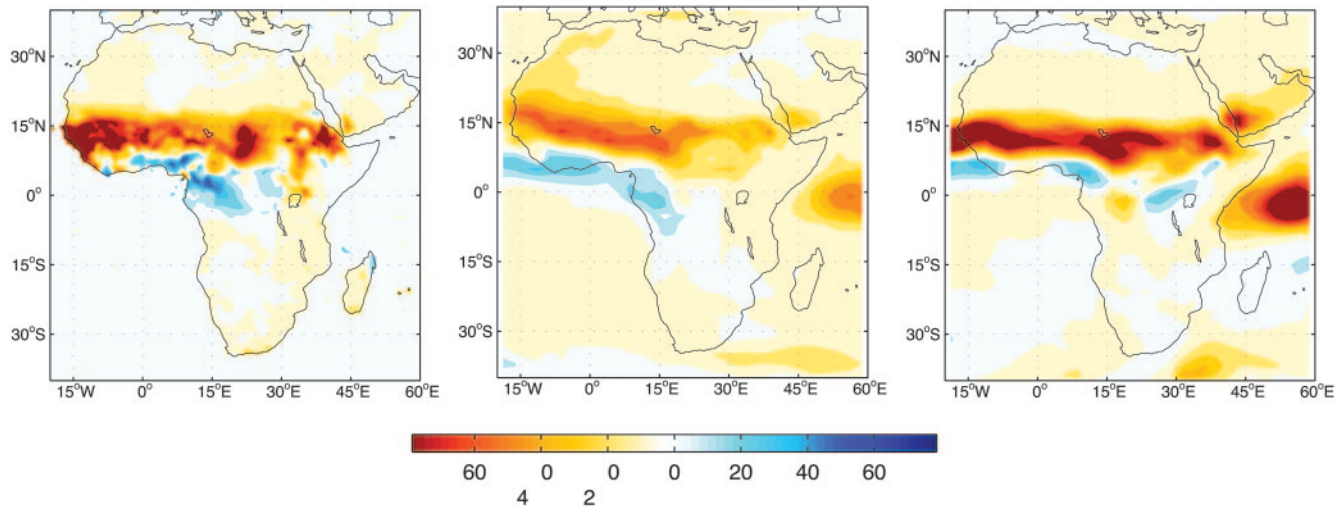

Fig. 2. Observed and modeled rainfall trends. (*Left*) The linear trend from 1950 to 2000 in the observed (CRU) July–August–September rainfall over land, in mm/month per 50 years. Blue areas correspond to a trend toward wetter conditions, and brown areas toward a drier climate. (*Center*) The linear trend for the eight-member ensemble mean of CM2 but plotted over both land and ocean. (*Right*) Linear trend for an ensemble mean of 10 simulations with the atmospheric/land component of CM2.0 running over observed sea surface boundary conditions.

comparable in timing and intensity to those observed in the 1970s and 1980s, but none of the runs captures the strength of the observed maximum in rainfall in the 1950s. From the perspective of these time series in isolation, we conclude that CM2's 20th century simulations are marginally consistent with the observations, with the realization that most resembles the observed time series being the driest member of the ensemble in the 1980s. The model supports the hypothesis that the drought of the later part of the century was partly related to a forced drying trend and partly a consequence of internal variability that happened to reinforce this trend.

The decline in Sahel rainfall in the second half of the 20th century in the model's ensemble mean is the result of anthropogenic forcing. An ensemble of three CM2.1 runs with natural forcing (solar plus volcanic only) produces an insignificant trend. A variety of integrations examining the response to different components of the anthropogenic forcing are underway. Results to date indicate that aerosols and the well mixed greenhouse gases are of comparable importance for the drying trend, but the existing ensemble size does not permit a more quantitative estimate of their relative importance. The aerosol results are in qualitative agreement with ref. 14. Because we only model the direct effect of aerosols on radiative fluxes and not the indirect effects on clouds, we may be underestimating the size of the aerosol forcing. The fact that increasing greenhouse gases also tends to dry the Sahel in CM2 runs counter to the conventional wisdom that this effect should be to increase precipitation by warming the Northern hemisphere more rapidly than the Southern hemisphere.

Although our eight historical CM2 runs include estimates of historical changes in the properties of the land surface, we have yet to perform coupled model experiments in which the effects of these changes are isolated. However, we have performed preliminary tests in a simpler model in which the ocean component is replaced by a motionless slab with uniform heat capacity and specified air–sea heat flux adjustments that mimic the effects of oceanic heat transport, in which we study the response to the change in land surface properties imposed in the historical runs. The results indicate that the response to these changes in land surface properties is modest and primarily confined in our model to the West African coastal forests rather than the Sahel.

The spatial pattern of the precipitation trends from 1950 to 2000 is shown in Fig. 2 for the CRU observations (*Left*) and the eight-member ensemble mean with the full set of forcings (*Center*). The model captures the moistening near the Gulf of Guinea as well as the basic pattern of the drying but with the center of mass of the drying shifted northwest of that observed. As evident from Fig. 1, the amplitude of the ensemble mean drying is weaker than that observed. The spatial pattern in the realization shown in Fig. 1 that best fits the observed time series is similar in structure but ≈25% larger in amplitude than the pattern in Fig. 2*b* (data not shown).

Because variations in SSTs are thought to underlie the changes in Sahel rainfall, it is important to test a model by running it over the observed sea surface as a boundary condition. Lu and Delworth (12) have analyzed Sahel rainfall in a set of 10 simulations for the period 1950–2000, using the atmospheric component of CM2.0, in which only the SST and sea ice are modified after observations, with no changes in greenhouse gases, aerosols, solar irradiance, volcanoes, or land use. Given the observed SSTs, the model comes much closer than the freely evolving coupled model to capturing the full range of the rainfall reduction from the 1950s to the 1980s (Fig. 3). It also captures some of the year-to-year variability in recent years but with some disconcerting departures from observations in earlier periods, such as the very wet prediction for 1971. (In a freely running coupled model, there is no reason to expect correlation with observations on a yearly time scale, because the model's internal variability of SSTs will be uncorrelated with the observed internally generated variations; however, when one runs an atmospheric model over the observed SSTs, one can hope to simulate some of the year-to-year variability in tropical rainfall.) The ensemble mean linear trend map for rainfall over 1950–2000 from these integrations is shown in the right panel of Fig. 2. The atmosphere/land component of this model run over observed SSTs captures the spatial pattern of the rainfall trend with considerable fidelity.

To put the Sahel drying trend in the context of the trends over the entire African continent, we include in Fig. 4 plots identical to those in Fig. 2, except for the annual mean precipitation. The annual mean simultaneously captures the rainy season in different regions at different times of year. The drying trend in the Sahel over the last half of the 20th century has been accompa-

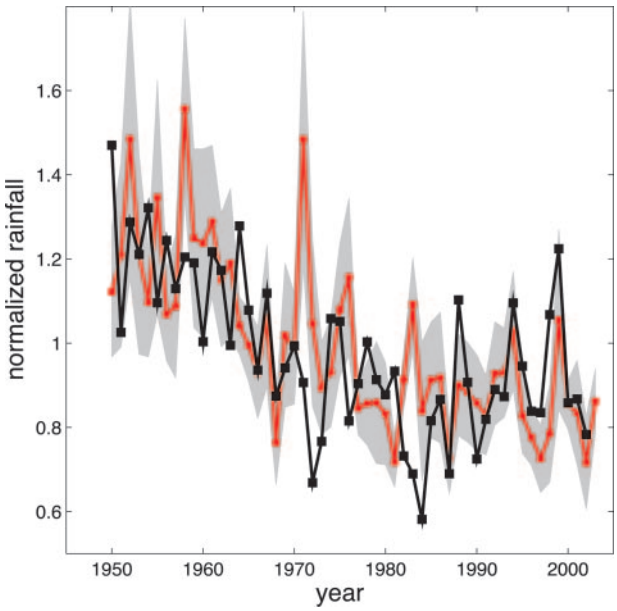

Fig. 3. Observed (CRU) Sahel July–August–September rainfall for each year (black), with no additional time smoothing, and ensemble mean of 10 realizations of the atmosphere/land component of CM2.0 (red) forced with observed ocean surface temperatures. Both are normalized to unit mean over 1950–2000. (This fixed SST model is 10% drier than the observations.) The gray area is ±1 standard deviation within the model ensemble.

nied by drying in southern Africa (13), whereas rainfall in parts of equatorial Africa has increased. The ensemble mean trend in CM2 is weak compared to that observed, and we have multiplied this trend by a factor of 2 in the plot to make the color range comparable to that observed. The spatial pattern of the ensemble mean trend does resemble the observations outside of the Sahel to the extent that it tends to dry in southern Africa near 15°S and to moisten most equatorial regions. Individual realizations have larger trends and show considerable variability in the pattern. The atmospheric model run over observed SSTs (Fig. 4 *Right*) generates stronger trends in general, including stronger drying in southern Africa.

The basic agreement between the model's 20th century African climate variations and observations has encouraged us to take a close look at the model's 21st century projections for the Sahel. (Projections for other parts of Africa will be discussed elsewhere.) In the first few decades of the 21st century (Fig. 1), there is some moistening or at least a cessation of the drying trend, but this is followed by rapid drying, with rainfall decreasing below that of the observed 1980s drought for the A1B and A2 scenarios. We suspect that the nonmonotonic behavior is related to structure in our imposed aerosol forcing. The spatial structure of this drying late in the 21st century (data not shown) is similar to the model result in Fig. 2, although the moistening along the Gulf of Guinea is less evident. The different scenarios sort themselves with time just as one would expect if (*i*) an increase in well mixed greenhouse gases causes the model's Sahel to dry and (*ii*) this increase is the dominant forcing agent in the 21st century.

This prediction differs from that of many other models, which often project little change or modest future increases in Sahel rainfall (17, 18). We have examined the new database of climate simulations collected for IPCC/AR4, based on 20 models from 14 modeling consortia. Although one model in the archive produces a 50% increase in July–August–September Sahel rainfall in the A1B scenario by 2100, a more typical result is a small increase of 0–15%. Four of the models other than CM2 produce small (5–15%) reductions in Sahel rainfall. CM2.0 and CM2.1 produce the strongest Sahel rainfall reduction in the 21st century of any of the models (≈25%). Nearly two-thirds of the models do hindcast a drying trend of at least 5% over the 20th century. Because most of these models do not continue the trend into the 21st century, the 20th century trends in most models are unlikely to be forced by greenhouse gases, with aerosol forcing being a more likely source.

We need to understand what it is within the formulation of CM2 that controls this response in the Sahel and causes it to differ from that in other models. Our analysis of CM2 supports the hypothesis that the evolution of SSTs controls much of the observed interannual variation of African rainfall. Given two models that predict different African climates for the 21st century, one should ask, first of all, whether this is because they predict different SSTs or whether they are responding differently to the same SSTs. We have confirmed that the latter is the case, based on a number of studies with the atmosphere/land component of the model, running over a variety of SST distributions, and with a model in which the ocean component is replaced by a motionless slab with constant heat capacity. CM2's 21st century response in the Sahel is not sensitive to differences in

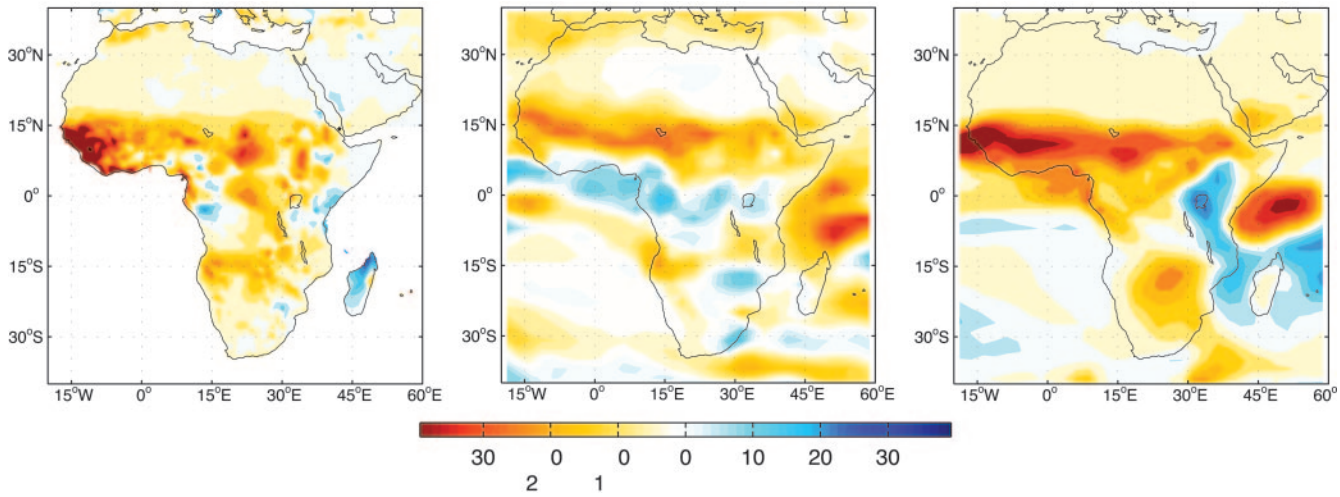

Fig. 4. As in Fig. 2 but for the annual mean precipitation. The CM2 ensemble mean trend in *Center* has been multiplied by 2.

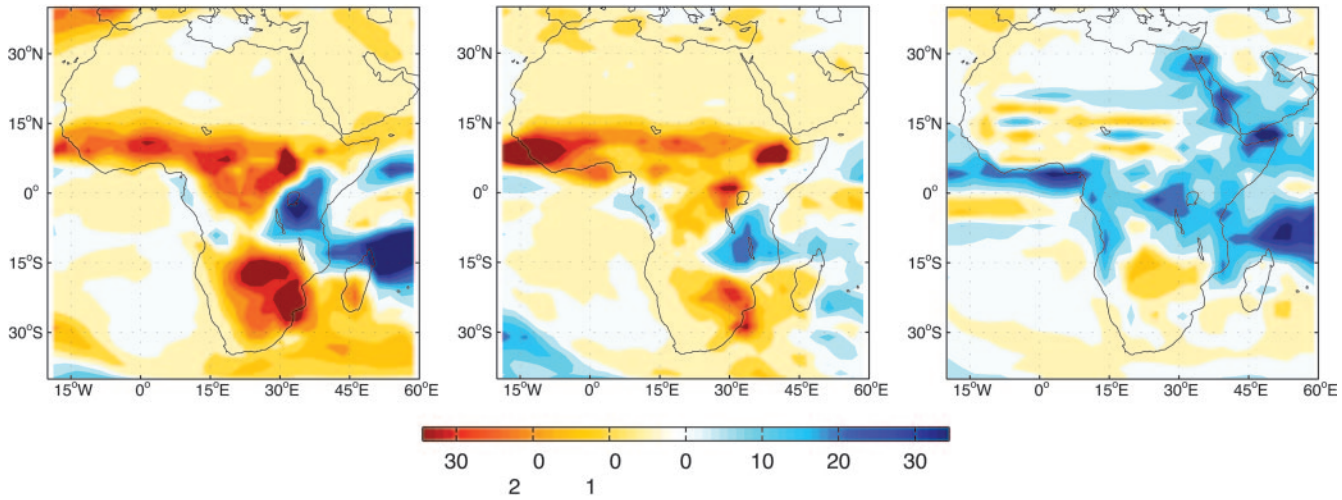

Fig. 5. The annual mean precipitation response of three atmospheric models to a uniform warming of ocean temperatures. (*Left*) The atmospheric component of CM2.0. (*Center*) A model developed at National Aeronautics and Space Administration's Global Modeling and Assimilation Office (J. Bacmeister, personal communication). (*Right*) The CAM3 model developed at the National Center for Atmospheric Research (J. Kiehl, personal communication).

spatial structure in the warming of SSTs of the magnitude typically predicted by different global warming models.

In perhaps the most informative of these computations, we have compared an integration of the atmosphere/land component of CM2.0 over observed climatological (seasonally varying) SSTs and sea ice with an integration in which the SSTs are uniformly increased over all ocean surfaces by 2 K. This uniform warming experiment has been performed by many other groups, as it is a standard point of comparison for cloud feedback studies (24, 25). In Fig. 5, we compare the CM2.0 response in annual mean precipitation over Africa with the responses in two other models. One is developed by the Global Modeling and Assimilation Office of National Aeronautics and Space Administration and used by ref. 10 in a study of 20th century Sahel rainfall. The other is the atmosphere/land component (CAM3) of the Community Climate System Model of the National Center for Atmospheric Research (26). Annual mean precipitation once again serves to highlight differences between the model responses in northern and southern Africa simultaneously. The CM2.0 response to uniform warming of the oceans is similar over the Sahel to that seen in its ensemble mean 20th century response in Fig. 4. GMAO has a qualitatively similar response. (To our knowledge, this model has not been used to simulate the 21st century.) CAM3's response is dramatically different, with moistening over much of Africa. The coupled model that incorporates CAM3 and is entered in the AR4 database (CCSM3.0) shows moistening over the Sahel in the 21st century. Yet this atmospheric model is one of those described in ref. 13 as simulating Sahel drying comparable to that observed over the past 50 years when run over the observed SSTs. Evidently, one can simulate the magnitude of this drying with models that possess very different sensitivities to uniform warming and to changes in temperature gradients. The uniform warming experiment isolates key differences between models in their simulations of African rainfall that are relevant for 21st century projections, and it should serve as a useful reference point in model comparison studies.

One must consider the possibility that Sahel rainfall responds not only to changes in SST gradients but also to a uniform warming of SSTs. A drying in response to uniform warming is the key not only to CM2's 21st century response but also to the contribution of greenhouse gases to its 20th century trend. The model's warming due to the well mixed greenhouse gases in the 20th century is not entirely uniform, with the Southern hemisphere warming more slowly than the Northern, as expected. But when the response to the uniform component of the warming is as large as in CM2, this component can evidently overcome the opposing effect of the changing SST gradients and change the sign of the response to increasing greenhouse gases.

Using the response of the atmospheric model to uniform warming of SSTs as a test bed, we have modified the model in a variety of ways to try to isolate the primary factor or factors controlling the response over the Sahel. The land surface model and the cloud prediction scheme have been our main foci. One conclusion is that land surface feedbacks within the model are significant but do not determine the basic character of the response. Modeling assumptions that affect the amount of moisture in the soil are an important aspect of land models. If we fix the amount of moisture stored in the soil while warming the climate, the model produces the same pattern of reduced rainfall in the Sahel and increased rainfall along the Gulf of Guinea as in Fig. 2, but with the latter increase amplified. Allowing the soil moisture to respond weakens the coastal moistening. These changes in soil moisture are reversible, responding from year to year to the changing precipitation; reversibility distinguishes these changes from the kinds of land surface modification that underlie discussions of desertification.

Another conclusion is that cloud feedbacks do play a role determining the Sahel drying response in our model. Comparing the interannual variability of the model's clouds to observations therefore may provide a test of a key aspect of the model formulation.

Direct observational confirmation of CM2's sensitivity to uniform warming is difficult; a response to uniform warming that is large enough to dominate a model's 21st century projections is difficult to isolate from the observational record, given the presence of the large contribution from changing SST gradients. Figs. 1–4 provide our best evidence to date that a model that does dry the Sahel strongly in response to uniform warming can be broadly consistent with the 20th century record.

Conclusion

We have described a global climate model (CM2) that generates a simulation of the 20th century rainfall record in the Sahel generally consistent with observations. The model suggests that there has been an anthropogenic drying trend in this region, due partly to increased aerosol loading and partly to increased greenhouse gases, and that the observed 20th century record is

a superposition of this drying trend and large internal variability. The same model projects dramatic drying in the Sahel in the 21st century, using the standard IPCC scenarios. No other model in the IPCC/AR4 archive generates as strong a drying trend in the future. Until we better understand which aspects of the models account for the different responses in this region to warming of SSTs, and devise more definitive observational tests, we advise against basing assessments of future climate change in the Sahel on the results from any single model in isolation. In the interim, given the quality of CM2's simulation of the spatial structure and time evolution of rainfall variations in the Sahel in the 20th century, we believe that its prediction of a dramatic 21st century drying trend should be considered seriously as a possible future scenario.

Extensive data sets from most of the CM2 integrations described in this article are available at http://nomads.gfdl.noaa.gov.

This work would not have been possible without the support of numerous members of the Geophysical Fluid Dynamics Laboratory Model Development Teams, as well as the Modeling Services and Computing Services Groups. We also acknowledge the Program for Climate Model Diagnosis and Intercomparison (PCMDI) for collecting and archiving the IPCC/AR4 model data. Special thanks to J. Kiehl and J. Bacmeister for access to the data from the CAM3 and GMAO model results displayed in Fig. 5.

1. Dai, A., Lamb, P. J., Trenberth, K. E., Hulme, M., Jones, P. D. & Xie, P.-P. (2004) *Int. J. Climatol.* **24,** 1323–1331.
2. Charney, J. G. (1975) *Quart. J. R. Meteorol. Soc.* **101,** 193–202.
3. Nicholson, S. (2000) *Rev. Geophys.*, **38, 1,** 117–139.
4. Xue, Y. & Shukla, J. (1993) *J. Climate* **6,** 2232–2245.
5. Taylor, C. M., Lambin, E. F., Stephenne, N., Harding, R. J. & Essery, R. L. H. (2002) *J. Climate* **15,** 3615–3629.
6. Folland, C. K., Palmer, T. N. & Parker, D. E. (1986) *Nature* **320,** 602–607.
7. Palmer, T. N. (1986) *Nature* **320,** 251–253.
8. Rowell, D. P., Folland, C. K., Maskell, K. & Ward, M. N. (1995) *Quart. J. R. Meteorol. Soc.* **121,** 669–704.
9. Fontaine, B., Trzaska, S. & Janicot, S. (1998) *Climate Dyn.* **14,** 353–368.
10. Giannini, A., Saravanan, R. & Chang, P. (2003) *Science* **302,** 1027–1030.
11. Bader, J. & Latif, M. (2005) *J. Climate*, in press.
12. Lu, J. & Delworth, T. L. (2005) *Geophys. Res. Lett.*, in press.
13. Hoerling, M. P., Hurrell, J. W. & Eischeid, J. (2005) *J. Climate*, in press.
14. Rotstayn, L. D. & Lohmann, U. (2002) *J. Climate* **14,** 2103–2116.
15. Vizy, E. K. & Cook, K. H. (2000) *J. Climate* **14,** 795–821.
16. Bader, J. & Latif, M. (2003) *Geophys. Res. Lett.* **30,** 2165–2169.
17. Paeth, H. & Hense, A. (2004) *Climatic Change* **65,** 179–208.
18. Maynard, N. H., Royer, J. F. & Chauvin, F. (2002) *Climate Dyn.* **19,** 499–514.
19. Harsmaa, J., Selten, F., Weber, N. & Kliphuis, M. (2005) *Geophys. Res. Lett.*, in press.
20. Delworth, T. L., Broccoli, A. J., Rosati, A., Stouffer, R. J., Balaji, V., Beesley, J. A., Cooke, W. F., Dixon, K. W., Dunne, J., Dunne, K. A., *et al*. (2005) *J. Climate*, in press.
21. Knutson, T. R., Delworth, T. L., Dixon, K. W., Held, I. M., Lu, J., Ramaswamy, V., Schwarzkopf, M. D., Stenchikov, G. & Stouffer, R. J. (2005) *J. Climate*, in press.
22. Wittenberg, A. T., Rosati, A., Lau, N.-C. & Ploshay, J. (2005) *J. Climate*, in press.
23. Nakicenovic, N., Alcamo, J., Davis, G., de Vries, B., Fenhann, J., Gaffin, S., Gregory, K., Grübler, A., Jung, T. Y., Kram, T., *et al*. (2000) *Special Report on Emissions Scenarios of the Intergovernmental Panel on Climate Change*, eds. Nakicenovic, N. & Swart, R. (Cambridge Univ. Press, Cambridge, U.K.).
24. Cess, R. D., Potter, G. L., Blanchet, J. P., Boer, G. J., Ghan, S. J., Kiehl, J. T., Le Treut, H., Li, Z.-X., Liang, X.-Z., Mitchell, J. F. B., *et al*. (1989) *Science* **245,** 513–516.
25. Cess, R. D., Zhang, M. H., Ingram, W. J., Potter, G. L., Alekseev, V., Barker, H. W., Cohen-Solal, E., Colman, R. A., Dazlich, D. A., Del Genio, A. D., *et al.* (1996) *J. Geophys. Res.* **101,** 12791–12794.
26. Hurrell, J. W., Hack, J. J., Phillips, A. S., Caron, J. & Yin, J. (2005). *J. Climate*, in press.

Corrections

INAUGURAL ARTICLE, ENVIRONMENTAL SCIENCES. For the article "Simulation of Sahel drought in the 20th and 21st centuries," by I. M. Held, T. L. Delworth, J. Lu, K. L. Findell, and T. R. Knutson, which appeared in issue 50, December 13, 2005, of *Proc. Natl. Acad. Sci. USA* (**102,** 17891–17896; first published December 1, 2005; 10.1073/pnas.0509057102), the numerical scales corresponding to the color bars in Figs. 2, 4, and 5 appeared incorrectly, due to a printer's error. The corrected figures and their legends appear below.

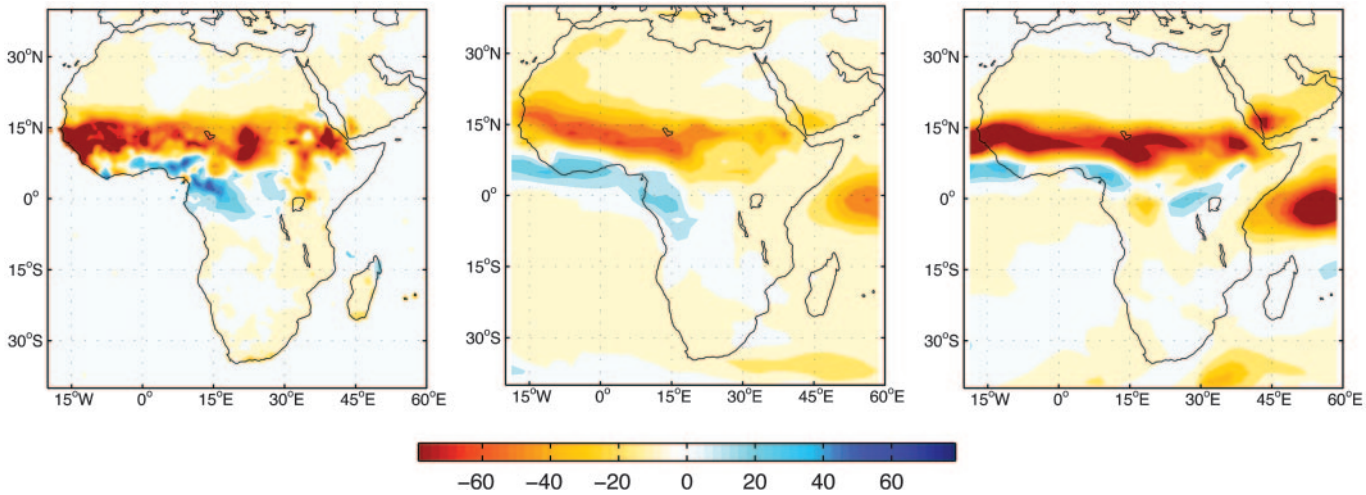

Fig. 2. Observed and modeled rainfall trends. (*Left*) The linear trend from 1950 to 2000 in the observed (CRU) July–August–September rainfall over land, in mm/month per 50 years. Blue areas correspond to a trend toward wetter conditions, and brown areas toward a drier climate. (*Center*) The linear trend for the eight-member ensemble mean of CM2 but plotted over both land and ocean. (*Right*) Linear trend for an ensemble mean of 10 simulations with the atmospheric/land component of CM2.0 running over observed sea surface boundary conditions.

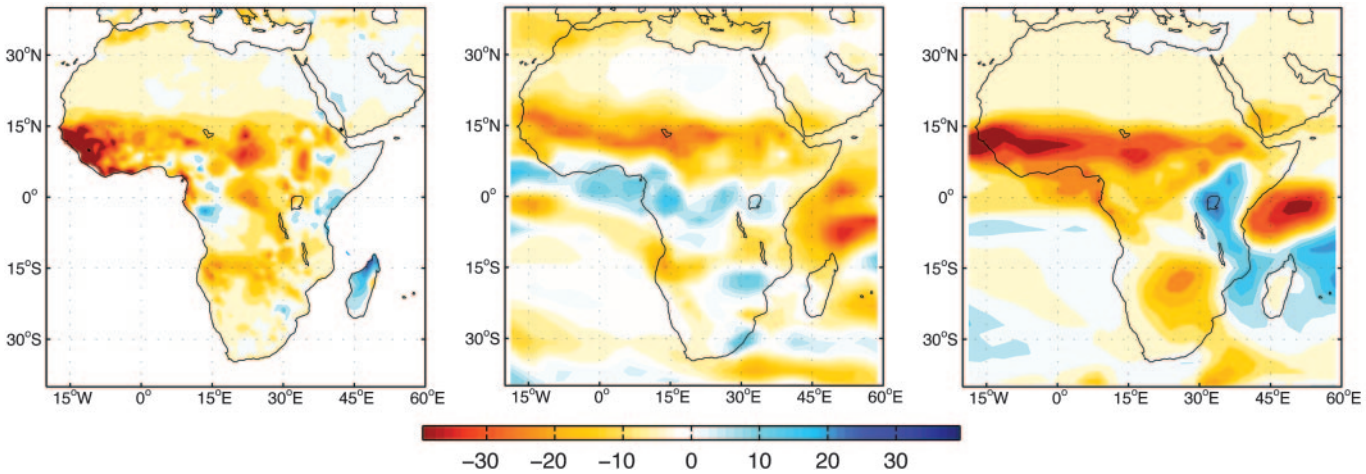

Fig. 4. As in Fig. 2 but for the annual mean precipitation. The CM2 ensemble mean trend in *Center* has been multiplied by 2.

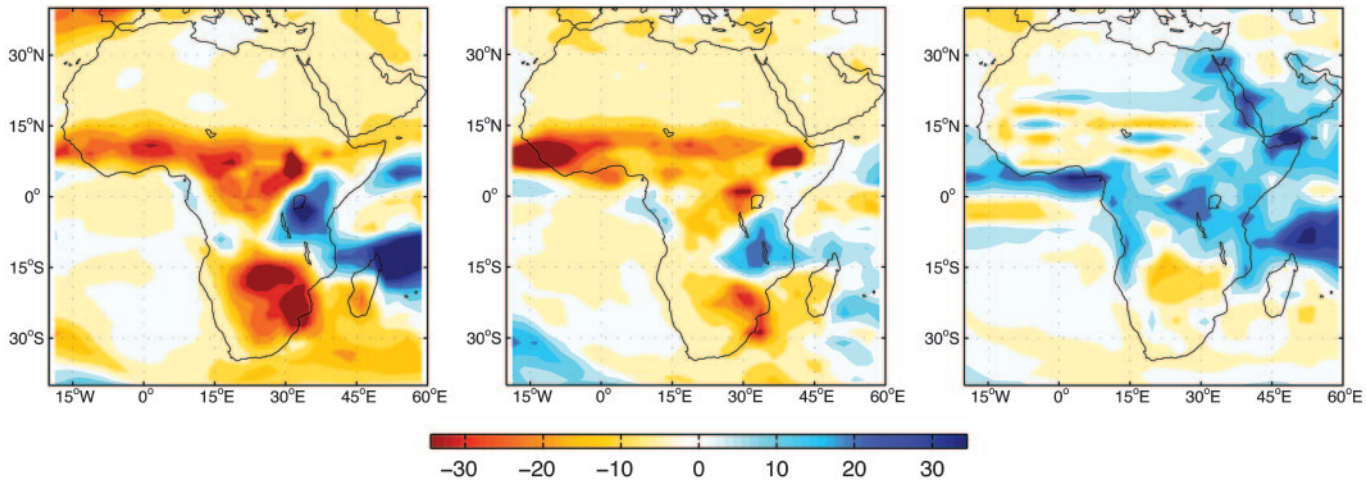

Fig. 5. The annual mean precipitation response of three atmospheric models to a uniform warming of ocean temperatures. (*Left*) The atmospheric component of CM2.0. (*Center*) A model developed at National Aeronautics and Space Administration's Global Modeling and Assimilation Office (J. Bacmeister, personal communication). (*Right*) The CAM3 model developed at the National Center for Atmospheric Research (J. Kiehl, personal communication).

www.pnas.org/cgi/doi/10.1073/pnas.0510844103

BIOCHEMISTRY. For the article "Multiple modes of interaction of the deglycosylation enzyme, mouse peptide *N*-glycanase, with the proteasome," by Guangtao Li, Xiaoke Zhou, Gang Zhao, Hermann Schindelin, and William J. Lennarz, which appeared in issue 44, November 1, 2005, of *Proc. Natl. Acad. Sci. USA* (**102,** 15809–15814; first published October 25, 2005; 10.1073/pnas.0507155102), the authors note that the horizontal labels for His-6-mPNGase and His-6-p97 in Fig. 5 are transposed. The corrected figure and its legend appear below.

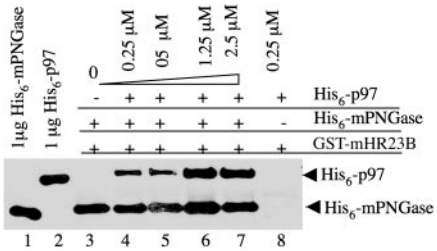

Fig. 5. mHR23B, mPNGase, and p97 form a complex. GSH-agarose beads (8 μl) containing 0.25 μM bound GST-mHR23B were incubated with 0.25 μM His-6-mPNGase in the presence of 0, 1, 2, 5, or 10 molar excess of His-6-p97. The samples were eluted in 45 μl of SDS-loading buffer and subjected to SDS/PAGE, electrotransferred, and then blotted with anti-His mAb.

www.pnas.org/cgi/doi/10.1073/pnas.0510409102

CELL BIOLOGY. For the article "Abnormal centrosome amplification in cells through the targeting of Ran-binding protein-1 by the human T cell leukemia virus type-1 Tax oncoprotein," by Jean-Marie Peloponese, Jr., Kerstin Haller, Akiko Miyazato, and Kuan-Teh Jeang, which appeared in issue 52, December 27, 2005, of *Proc. Natl. Acad. Sci. USA* (**102,** 18974–18979; first published December 19, 2005; 10.1073/pnas.0506659103), the authors note that the following statement should be added to the Acknowledgments: "We thank Dr. Patrizia Lavia (National Research Council Center of Evolutionary Genetics, University of Rome) for the generous gift of the RanBP1HA plasmid."

www.pnas.org/cgi/doi/10.1073/pnas.0511236103